Cellulose (2013) 20 807–818
DOI 10.1007/s10570-013-9867-9

ORIGINAL PAPER

Mechanical deconstruction of lignocellulose cell walls and their enzymatic saccharification

Ingrid C. Hoeger · Sandeep S. Nair · Arthur J. Ragauskas · Yulin Deng · Orlando J. Rojas · J. Y. Zhu

Received: 3 November 2012/Accepted: 15 January 2013/Published online: 24 January 2013

Abstract Laboratory mechanical softwood pulps (MSP) and commercial bleached softwood kraft pulps (BSKP) were mechanically fibrillated by stone grinding with a SuperMassColloider®. The extent of fibrillation was evaluated by SEM imaging, water retention value (WRV) and cellulase adsorption. Both lignin content and mechanical treatment significantly affected deconstruction and enzymatic saccharification of fibrillated MSP and BSKP. Fibrillation of MSP and BSKP cell walls occurs rapidly and then levels off; further fibrillation has only limited effect on cell wall breakdown as measured by water retention value and cellulase adsorption. Complete (100 %) saccharification can be achieved at cellulase loading of 5 FPU/g glucan for BSKP after only 15 min fibrillation with energy input of 0.69 MJ/kg. However, the presence of lignin in MSP affects the extent of fibrillation producing fibrils mainly above 1 μm. Lignin binds nonproductively to cellulases and blocks cellulose thereby reducing its accessibility. As a result, the cellulose saccharification efficiency of MSP fibrils (6 h of fibrillation, energy input of 13.33 MJ/kg) was only 55 % at same cellulase loading of 5 FPU/g glucan.

Keywords Cell wall deconstruction · Enzymatic hydrolysis · Saccharification · Lignocelluloses · Size reduction · Grinding · Nanocellulose · Nanofibers · Nanofibrils · Lignocellulose nanofibrils · Biofuel

This work is conducted on official government time of Zhu while Hoeger and Nair were visiting scientists at the USDA Forest Service, Forest Products Laboratory.

I. C. Hoeger · O. J. Rojas
Department of Forest Biomaterials, North Carolina State University, Raleigh, NC, USA

S. S. Nair · A. J. Ragauskas · Y. Deng
Institute of Paper Science and Technology, Georgia Institute of Technology, Atlanta, GA, USA

A. J. Ragauskas
Department of Chemistry and Biochemistry, Georgia Institute of Technology, Atlanta, GA, USA

Y. Deng
Department of Chemical and Biomolecular Engineering, Georgia Institute of Technology, Atlanta, GA, USA

J. Y. Zhu (✉)
USDA Forest Service, Forest Products Laboratory, Madison, Wl, USA
e-mail: jzhu@fs.fed.us

Introduction

Lignocellulose is the most abundant renewable material on earth (Perlack et al. 2005). Traditional utilizations of lignocelluloses include structure materials, hog fuel, and paper fibers. Proper deconstruction or fractionation of cell wall components can facilitate the development of a variety of high value materials. For example, structural carbohydrates can be enzymatically saccharified to monomeric sugars which can be used as building blocks to produce biofuels and a variety of chemicals (Bozell

and Petersen 2010). However, a pretreatment step such as dilute acid (Sun and Cheng 2002), ammonia (Gupta and Lee 2009), Alkaline green liquor (Koo et al. 2011), SPORL (Zhu et al. 2009b), etc., is required to remove the natural resistance of lignocellulose cell wall to microbial deconstruction — recalcitrance (Himmel et al. 2007; Zhu et al. 2011b) for efficient enzymatic saccharification. Conventional physical pretreatment through mechanical size reduction of lignocelluloses to the level of fiber or fiber bundles--Class I size reduction (Leu and Zhu 2012) has always been applied in conjunction with a thermo-chemical pretreatment but it is not capable of achieving good saccharification when applied alone (Zhu et al. 2009a; Zhu 2011). Mechanical size reduction can proceed beyond Class I size reduction resulting in complete breakup of the cell wall to micro- or nano-fibrils--Class II size reduction (Leu and Zhu 2012)—to achieve complete saccharification without thermo-chemical pretreatment. Conclusions similar to the class II size reduction concept and the efficacy of breakdown cell wall to nanofibrils for complete saccharification of wood cellulose were also reported by Endo and co-workers (Endo 2010; Lee et al. 2010). Although mechanical energy consumption is very high for Class II size reduction, it can avoid undesirable compounds produced in thermo-chemical pretreatment and thereby facilitate downstream processing. It also can produce a very pure and chemically unmodified lignin for value-added co-product development. Therefore, evaluation of mechanical cell wall deconstruction through Class II size reduction has practical significance.

This study evaluates the direct enzymatic saccharification of fibrils produced by Class II size reduction of chemical and mechanical softwood pulps using a commercial stone disk grinder. Similar evaluation using hardwood was conducted by Endo (2010); however, the fiber source used in the present investigation (softwoods) is much more recalcitrant and with higher lignin content than hardwood. Such evaluation is different from studies of the dynamics of enzymatic hydrolysis of nanofibrillated cellulose films produced from bleached and unbleached kraft birch fibers with very low lignin content (Ahola et al. 2008; Martin-Sampedro et al. 2012). Such evaluation is also different from those studies that carried out wood size reduction after thermochemical pretreatment of wood chips, such as alkaline green liquor (Koo et al. 2011), sodium hydroxide (Zhu et al. 2009a), hot compressed water (Lee et al. 2010), dilute acid and SPORL (Zhu et al. 2010), that removed a significant amount of cell wall components to enhance enzymatic saccharification. The objective of this study is to uncover the relationship among the degree of mechanical fibrillation, the associated energy consumption and the enzymatic digestibility of fibrillated lignocellulose fibrils. We also examined the effect of lignin removal on enzymatic saccharification by comparing fibrils produced from BSKP and MSP sources.

Materials and methods

A bleached softwood (loblolly pine) kraft dry lap pulp sample (BSKP) was obtained from a commercial source. The chemical composition of the BSKP is listed in Table 1. A sample of lodgepole pine was used to produce laboratory mechanical pulp. The sample was harvested from the Sulphur Ranger District, Arapaho–Roosevelt National Forest, Colorado, as described previously (Luo et al. 2010; Zhu et al. 2011a). The trees were about 100 years old, with a diameter of approximately 25 cm at breast height; the logs were debarked at site and then wrapped in plastic bags and shipped to USDA Forest Service, Forest Products Laboratory, Madison, Wisconsin. The wood logs were then chipped and the wood chips were screened to remove all particles greater than 38 mm and less than 6 mm in length. The accepted chips had a thickness range from 3 to 8 mm.

Endoglucanase (Fibercare®), and a mixture of cellulases (Cellic CTec2) with an activity of approximately 150 FPU/mL were kindly provided by Novozymes North America (Franklinton, NC). All other chemicals used were ACS reagent grade from Sigma to Aldrich (St. Louis, MO).

Table 1 Chemical compositions of the bleached softwood kraft pulp (BSKP) and mechanical softwood pulp (MSP)

	Klason lignin (%)	Arabinan (%)	Glactan (%)	Glucan (%)	Xylan (%)	Mannan (%)
BSKP	0.2	0.6	0.3	79.6	9.2	5.9
MSP	29.2	2.1	4.2	39.1	6.0	10.0

Mechanical pulping of lodgepole pine chips

The lodgepole pine wood chips were pre-steamed (Andritz Sprout-Bauer Atmospheric Refiner, Springfield, OH) for 10 min to increase their moisture. The chips were refined in a mechanical refiner (Sprout–Waldron Operation, Koppers Company, Muncy, PA) operating at atmospheric pressure. The two disk-platesin the refiner have a D2-B505 pattern. The disk plate gap used in the first pass was 0.51 and 0.18 mm in the second pass. A vibratory screen (Cooper Crouse-Hinds, Houston, Texas) with mesh opening size of 0.15 mm was used toremovefiber bundles. The obtained fiber suspension is denoted here as Mechanical Softwood Pulp (MSP).

Mechanical nanofibrillation

The BSKP sample at 2 % solids was soaked in deionized water for 24 hand then disintegrated using a lab disintegrator (TMI, Ronkonkoma, NY) after 10,000 revolutions before mechanical fibrillation using a SuperMassColloider (Model MKZA6-2, DISK Model: MKGA6-80#, Masuko Sangyo Co., Ltd, Japan). The MSP sample was used directly after refining and screening for similar mechanical fibrillation, using the SuperMassColloider. As described previously (Wang et al. 2012b), pulp was fed continuously by gravity to the Colloider consisting of two stone grinding disks rotating at 1,500 rpm. The gap of the two disks was set at −100μm. The zero gap was determined right at the contact position before loading pulp. The presence of pulp between the disks ensured that there was no direct contact between the two disks even at the negative setting. Fibrillated samples were collected periodically and the time–dependent energy consumption was recorded using a power meter (Model KWH-3 Energy Meter, Load Control Inc., Sturbridge, MA). To avoid mold growth the samples were treated with Kathon CP/ICP II (Rohm and Haas company, Bellefonte, PA) at a dose of 10 μL/mL of the fibrillated suspension.

Characterization of the nanofibrillated material

Water retention values (WRV)

Water retention value (WRV) was used to indirectly asses the total internal pore and interfibril surface areas and substrate accessibility to cellulase (Luo and Zhu 2011). A modification of the TAPPI standard Method 256 (TAPPI 2009) was used to determine WRV for both of the unfibrillated pulp and the fibrillated sample. Samples at 4 % solids, with an oven dry (od) weight of 0.25 g, were centrifuged at 900*g* for 30 min (Model EXD, International equipment CO, Boston, MA). The samples were weighed and oven dried at 105 °C until reaching a constant weight. The WRV was determined as the amount of water held by the fibers/fibrils upon centrifugation relative to the od weight of the substrate.

Characterization ofcellulose nanofibrils (CNF) from BKSP

The morphology of lignin free cellulose nanofibrils (CNF) from BSKP was analyzed by scanning electron microscope (LEO EVO 40 SEM, Carl Zeiss NTS, Peabody, Massachusetts) at 15 kV. Drops of the NFC sample at approximately 0.1 % consistency were dried on polished aluminum mounts and were sputter-coated with gold to provide adequate conductivity.

The CNF crystallinity was measured by a FT-Raman spectroscopic method (Agarwal et al. 2010) using approximately 0.15 g of air-dried sample pressed into a pellet with a Bruker MultiRam spectrometer (Bruker Instruments Inc., Billerica, MA). Crystallinity index was calculated using the Raman spectral intensities at two wavenumbers (cm^{-1}) as

$$\mathrm{Cr}_{\mathrm{Raman}} = [(I_{380}/I_{1096}) - 0.0286]/0.0065 \quad (1)$$

Characterization of lignocellulose nanofibrils (LCNF) from MSP

The morphology of the lignocellulose nanofibrils (LCNF) was analyzed by field emission scanning electron microscope (FE-SEM, JEOL, 6400F, Peabody, MA, USA) operating at 10 kV. Drops of LCNF suspension at approximately 0.1 % consistency were air dry onto clean silicon wafers and then fixed on carbon tape and coated with a layer of Au/Pt. The diameter distribution was obtained from at least 300 fibers or fibrils randomly selected and the image analyzed using a Revolution software (4pi Analysis Inc. Durham, NC). The crystallinity of the LCNF samples were determined by X-ray diffraction with a diffractomerter (Rigaku SmatLab) equipped with a monochromater using a Cu Kŭradiation at 40 kV and

44 mA. The scans were performed 5–50° 28 with a step size of 0.05° and a count time of 15 s at each step. The crystallinity was calculated using the Segal method (Segal et al. 1959) with the (002) crystal plane corresponding to 22.5° (2d) and after subtracting the amorphous contribution at 21° (2d):

$$\text{Crystallinity} = \left[1 - \left(I_{\text{amorphous}}/I_{[002]}\right)\right] \times 100 \quad (2)$$

Cellulose accessibility

Cellulose accessibility to cellulase for each fibrillated sample was evaluated from the extent of endoglucanase binding. A commercial grade endoglucanase, Fibercare® was used and its concentration in the suspension was determined by UV–Visspectrometry (Liu et al. 2011; Wang et al. 2012a). Each sample of 0.1 g was treated with endoglucanase loading equivalent to 50 mg protein/L in 110 mL of acetate buffer (pH 4.8) at 4 °C. The sample suspension was circulated through a quartz cuvette of 10 mm optical path length using a flow loop and a peristaltic pump as describe previously (Liu et al. 2011). The free enzyme concentration in the solution was continuously monitored by a UV–Vis spectrometer (Model 8453 Agilent, Palo Alto, CA) at wavelength 291 nm. The second derivate method was applied to correct for spectral interferences from light scattering by small particles and absorption by any lignin leached during the experiments (Chai et al. 2001; Liu et al. 2011).

Enzymatic saccharification of CNF and LCNF

Enzymatic hydrolysis experiments were carried out at a substrate solids consistency of 1 % (w/v) in sodium acetate buffer of pH 4.8 at 50 °C in an incubator (Excella E25, New Brunswick Scientific, Edison, NJ) at 200 rpm. A commercial cellulase cocktail (CTec2) at different loadings of 2, 5, 10 and 15 FPU/g glucan was used. Hydrolysates were sampled periodically at 0.5, 1, 2, 3, 5, 7, 9, 24, and 48 h for glucose analysis. The aliquots were centrifuged at 12,000 rpm (Sorvall Legend Micro 17 centrifuge, ThermoFisher Scientific) for 5 min, and the glucose in the supernatant was measured using a biochemistry analyzer (YSI 2700, YSI Incorporated, Yellow Springs, OH). The substrate enzymatic digestibility (SED), defined as the percent of glucan in the solid substrate enzymatically saccharified to glucose, was used to represent cellulose saccharification efficiency.

Results and discussion

Mechanical breakdown of cell wall: SEM imaging

The systematic physical breakdown of the cell wall of BSKP samples is evident from SEM images obtained before (Fig. la) and after 6 h fibrillation (Fig. 1b). The BSKP fibers have an average width of approximately 40 µm, while most of the fibers were highly fibrillated to micro or nanofibrils after 6 h of fibrillation by the SuperMassColloider. The gradual fibrillation of the BSKP can be observed from Fig. 1c–h corresponding to samples obtained after different fibrillation times. Copious amounts of original BSKP fibers, 20-40 µm diameter, remained after 15–30min fibrillation. These fibers were only externally fibrillated and produced hairy features or fibrils that unravel from the external surface. However, the fiber number density was reduced and the respective widths became smaller as fibrillation continued (compare Fig. 1a, g). Further fibrillation produced size reduction beyond the fiber level, to the submicron and nanofibril levels, which can be clearly observed from high resolution SEM images (Fig. 1d, f, h). Negligible variations in fiber morphology were noted with continued fibrillation (beyond 1 h), at least as indicated by SEM imaging (compare Fig. 1b, h). The fibril morphology shown in these SEM images is in agreement with those reported in the literature (Henriksson et al. 2008; Iwamoto et al. 2007).

The gradual breakdown of fiber cell wall and the reduction in fiber dimensions through mechanical fibrillation was also observed upon grinding MSP (Fig. 2). Microfibrils were released through the mechanism of internal mechanical fibrillation (Dekker 2003; Hartman 1985; Kerekes 2005) as can be observed from the reduction in the diameter of the fibers, down to a few micrometers or smaller. It appears that the reduction in fiber diameter was rapid as can be observed in Fig. 2. Fibers with size similar to that of the original fibers were observed in early stages of the mechanical fibrillation (Fig. 2b), in agreement with observations from BSKP (Fig. 1c and e).

Pits were fairly resistant to fibrillation (Siwiö and Kärenlampil 1998). Furthermore, while fiber swelling favors fibrillation (Besbes et al. 2011), water-resistant pits produce the opposite effect. Therefore, it is interesting to note that pit fragments were clearly visible after 1 h fibrillation (Fig. 2c). Finally, after

fibrillation for 6 h, the microfibers reached a fairly uniform diameter, which can be confirmed by the narrow diameter distribution around 1.75 μm (Fig. 2d, e).

Interestingly, the energy consumption of mechanical fibrillation by the SuperMassColloider was found to depend on the fibrillation time alone and independent of the chemical composition of the fibers. The

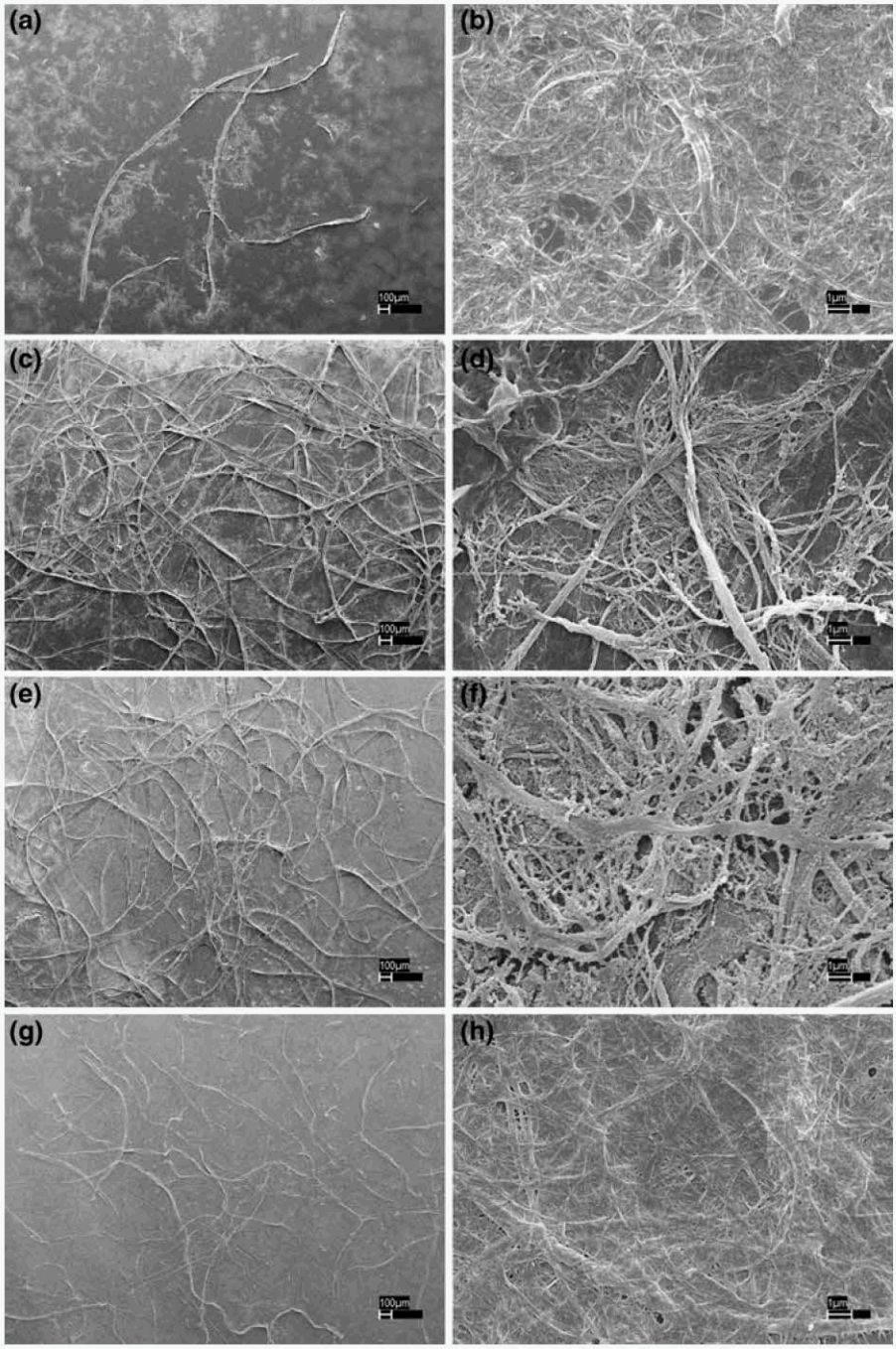

Fig. 1 SEM images of BSKP at different fibrillation times: **a** 0 h; **b** 6 h; **c**, **d** 0.25 h; **e**, **f** 0.5 h; **g**, **h** 1 h. Note the difference of the *scale bars*, 100 μm for **a**, **c**, **e**, and **g**; 1 μm for **b**, **d**, **f**, and **h**

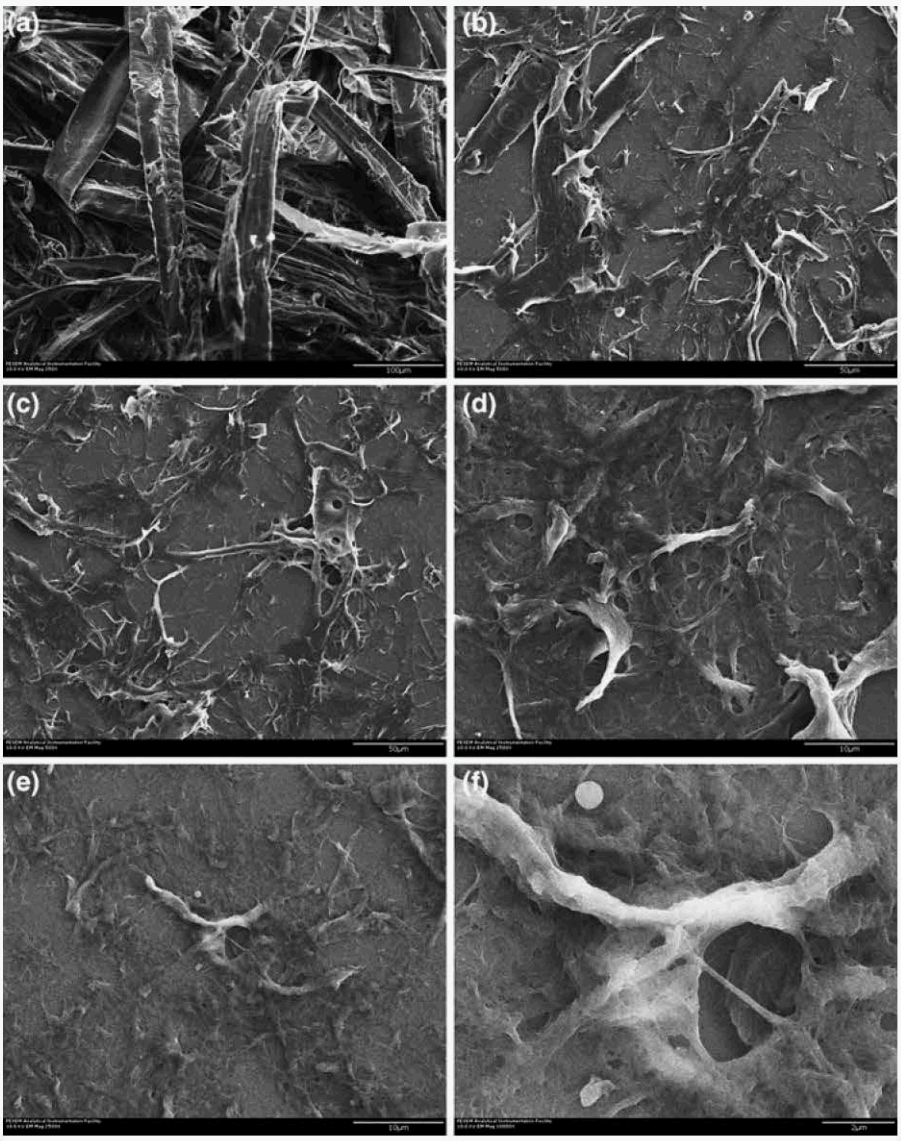

Fig. 2 FE-SEM images of MSP after different fibrillation times: **a** 0 h "initial pulp", *scale bar* 100 μm; **b** 0.25 h, *scale bar* 50 μm; **c** 1 h, *scale bar* 100 μm; **d** 6 h, *scale bar* 10 μm; **e** 9 h, *scale bar* 10 μm; **f** close up of 9 h, *scale bar* 2 μm

fibrillation energy consumed during processing of BSKP and MSP fits a linear relationship: energy (MJ/kg) = 2.1(MJ/kg h) × time (h), $r^2 = 0.998$ (Fig. 3a, b). It is interesting to note that despite the differences in fiber source and chemical composition the energy consumed was the same for BSKP and MSP; for example, approximately 14 MJ/kg were consumed after 6 h BSKP and MSP fibrillation. However, what distinguish these two fiber sources is that the degree of fibrillation was quite different (Figs. 1, 2), i.e., more nanofibrils were produced from BSKP than from MSP. This observation contradict to that reported previously that suggested fibrillation of lignin-containing pulps produced finer fibrils when unbleached kraft pulp with very low lignin content was used (Spence et al. 2011).

The breakdown of cell wall can also be observed from the manually measured distribution of fibril diameters from the SEM images of the MSP sample (Fig. 4). The original MSP sample has two peaks in the diameter distribution probability density curve. The peak at approximately 1–2 μm was from the fines

produced from mechanical refining during producing MSP. The second peak at approximately 45 µm represents fiber diameter, as shown in Fig. 2a. With only 15 min fibrillation, the second peak disappeared and the distribution peaked at 0.75–1.75 µm, which suggests the MSP fibers were delaminated into macrofibrils of approximately 1 µm. However, fibers with diameter 5–35 µm still exist (Figs. 2b, 4). Continued fibrillation eliminated large fibrils, above 5 µm, resulting in fibrils with diameters between 0.75 and 1.75 µm (6 h data in Fig. 4). It appears that the selected stone disk (MKGA6-80#) in the SuperMass-Collider is not able to further break the crosslinked lignin barrier to produce fibrils with widths of <1 µm. This is quite evident from the fact that the fibril diameter distribution density below 1 µm was essentially unchanged even after 6 h fibrillation. This is also supported by SEM imaging (Fig. 2). The absence of lignin facilitated mechanical fibrillation of BSKP to produce fibrils with diameters in the nanoscale (Fig. 1), much smaller than those observed in Fig. 2 of MSP fibrils under same energy consumption.

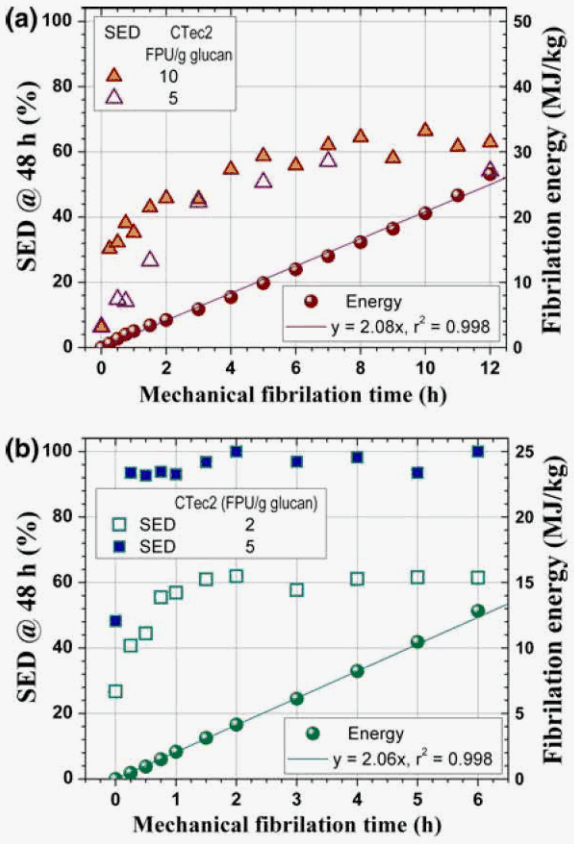

Fig. 3 Effect of fibrillation on enzymatic saccharification efficiency, represented by fibrillated substrate enzymatic digestibility (SED), and energy consumption for fibrillation. **a** MSP **b** BSKP

Degree of fiber fibrillation (cell wall breakdown)

Water retention value (WRV) is a measure of fiber swelling capacity. It quantifies the amount of water in fiber pores and between fibers after elimination (via centrifugation) of free water inside the cell lumen (Luo et al. 2011; Weise et al. 1996). WRV has been used to measure the degree of micro fibrillation or homogenization of cellulose (Cheng et al. 2007). WRV increased rapidly in the first hour of fibrillation for both the BSKP and MSP samples (Fig. 5). WVR reached a plateau for BSKP thereafter. This suggests that pores are almost completely accessible so that no more water-accessible surface can be created through continued fibrillation. This is corroborated by the similar morphologies of the fibrillated samples observed in SEM imaging (Fig. 1h, b). For the MSP sample, WRV continued to increase but much slowly after 1 h fibrillation (Fig. 5). WRV of the MSP sample is lower than that of the BSKP under the same fibrillation time. This indicates that the extent of fibrillation of BSKP is much severe than that of MSP at a given fibrillation time (see SEM images in Figs. 1h, 2c). Furthermore the cross-linked lignin in MSP sample is more hydrophobic and reduces fibril flexibility to swell. While the BSKP has good swelling and flexibility due to decreased heteropolysaccharides

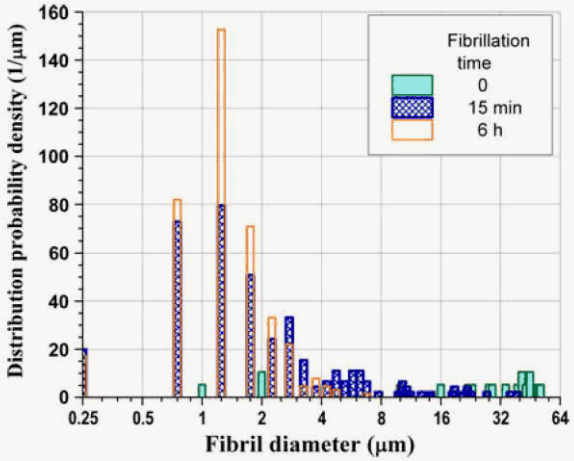

Fig. 4 Comparisons of MSP fibril diameter distribution probability density functions at three different fibrillation times

content which reduced the charge density of the fibers (Laine and Stenius 1997).

Overall, fibrillation reduces the crystallinity of the fibrils by about 15–25%. This is in agreement with other reports (Iwamoto et al. 2007). The continuous shearing by the grinding stones can destroy the cellulose crystals and shorten the chain length resulting in smaller crystals (Wang et al. 2012b). This can be seen from the measured crystallinity index of the BSKP fibrils (Fig. 6). The crystallinity index of the BSKP fibers was 57 % and reduced to approximately 46 % after 6 h fibrillation. The rate of reduction in crystallinity was rapid in the first 2 h and then decreased, suggesting the crystal structure of BSKP was well destroyed in early stage of fibrillation. The measured crystallinity index of the MSP fibers was only 47 % due to the presence of a significant amount of lignin (29.2 %)that is amorphous. Furthermore, the rate of reduction in crystallinity index was slow in the early stage of fibrillation, but increased after 4 h fibrillation. This is opposite to that observed from MSKP and suggests that mechanical fibrillation energy was used to breakdown the crosslinked lignin and hemicelluloses in the early stage fibrillation. The cellulose crystal structure can then be rapidly destroyed.

Enzymatic hydrolysis of nanofibrillated BSKP and MSP

It is known that mechanical size reduction can enhance enzymatic saccharification of lignocellulosic substrates (Dasari and Berson 2007; Zhu et al. 2009a, 2010). However, most studies that use conventional size reduction resulted in two main conclusions: (1) there is a significant effect of substrate size but limited maximal saccharification when using a lignocellulose that is not thermo-chemically or biologically treated or modified (Dasari and Berson 2007; Zhu et al. 2009a); (2) there is a limited or reduced effect of size reduction but with significant saccharification efficiency, e.g., 50 % or high, when using fairly well pretreated substrates, for example, by dilute acid, sulfite, organosolv (Zhu et al. 2010). In a previous study, we proposed the concept of two classes of plant biomass size reduction (Leu and Zhu 2012). Class I merely increases the external surface area by producing fibers or fiber bundles without significant breakup of fiber cell walls. Class II completely breaks down fibers to render cell walls fully accessible to enzymes. The efficacy of Class II size reduction for enzymatic saccharification of untreated wood was corroborated by Endo using direct milling of Eucalyptus wood powder (Endo 2010). Solid-state NMR measurements indicated the domain (fibril) size was approximately 5 nm in the Eucalyptus milled substrate. However, the SEM images of the milled softwood pulps shown in Figs. 1 and 2 indicate both Class I and Class II size reduction with fibril size bigger than 5 nm. This discrepancy is partly due to the indirect NMR method used by Endo (Endo 2010). The effect of the two classes of size reduction on wood cellulose saccharification can be clearly observed from the enzymatic hydrolysis of the MSP fibrils. The MSP was produced

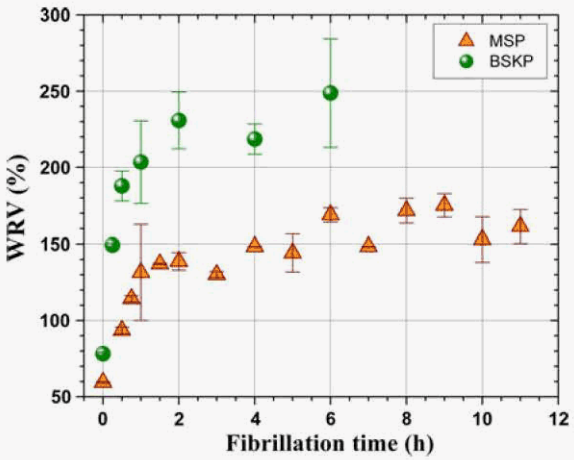

Fig. 5 Effect of fibrillation time on water retention values (WRVs) of BSKP and MSP

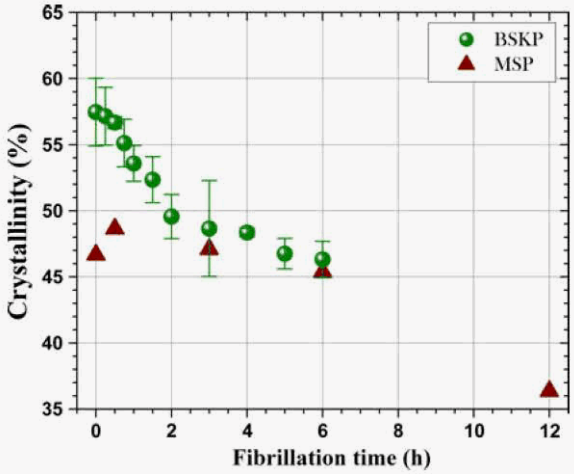

Fig. 6 Effect of fibrillation time on crystallinities of BSKP and MSP

from mechanical pulping of lodgepole pine wood chips without any thermo-chemical pretreatment, as described in the materials and methods section. The cellulose enzymatic saccharification efficiency of MSP at cellulase loading of 10 FPU/g glucan, represented by SED, was only approximately 6 % without mechanical fibrillation by the SuperMassColloider (Fig. 3a). SED was significantly increased by fivefold, to 30 % after just 15 min fibrillation time (Class I size reduction). The Class I size reduction enables significant increase in hydrolysis, but only reached unsatisfactory SED of 30 %. SEM images indicated that the cell wall was only partially broken and large fibers were still visible (Figs. 2b and 4). Continued increase in SED was observed with further fibrillation--Class II size reduction. SED approached 60 % after fibrillation for 6 h. The fibers were completely fibrillated to become macrofibrils (Fig. 2d). Even at cellulase loading of 5 FPU/g glucan, a SED of 60 % after 48 h hydrolysis was achieved for samples fibrillated for 6 h. A cellulase loading of 5 FPU/g glucan is low compared to cellulase loading reportedin most studies using softwoods. This suggests that efficient saccharification of untreated softwood is possible at relatively low cellulase loadings without any thermo-chemical pretreatments by using mechanical fibrillation alone when the cell wall is completely broken down to nanofibrils, agree with those reported by Endo using a Eucalyptus (hardwood) (Endo 2010). This verifies the concept of Class II size reduction to reconcile conflicting results reported in the literature on the effect of plant biomass size reduction on enzymatic saccharification.

BSKP was produced through chemical pulping and bleaching. However, the effect of mechanical fibrillation on enzymatic saccharification of BSKP showed similar results as discussed above for MSP (Fig. 3b). At a cellulase loading of only 2 FPU/g glucan, SED was increased from approximately 27−60 % after 1 h fibrillation with most fibers fibrillated into nanofibrils (Fig. 1g, h) and render fiber cell wall completely accessible to cellulase. SED at 48 h was 94 % with only 15 min fibrillation at cellulase loading of 5 FPU/g glucan. The difference in cellulose saccharification at the same cellulase loading of 5 FPU/g glucan between fibrillated BSKP and fibrillated MSP is primarily a result of nonproductive cellulase binding to lignin (in MSP fibrils) (Lan and Zhu 2012; Mansfield et al. 1999; Sewalt et al. 1997) and lignin blockage or coverage effect (Mansfield et al. 1999; Wang et al. 2012c) to reduce cellulose accessibility to cellulase. Spherical particles were observed in the MSP fibrils (Fig 3f). These particles most likely are Pseudo-lignin. It is possible that the separated amorphous lignin by mechanical grinding in the SuperMassCollider can be agglomerated and re-precipitated (Hu et al. 2012; Kallavus and Gravitis 1995). The unseparated lignin can cover the cellulose microfibrils as hypothesized by Endo and co-workers (Lee et al. 2010). These phenomena will affect cellulose accessibility.

The above mechanistic discussions of the effects of two classes of size reduction on enzymatic saccharification can be supported by quantitative measurements. Mechanical fibrillation breaks down cell walls and increases cellulose accessibility as can be seen from the increase in the amounts of cellulase bound with fibrillation time (Fig. 7). The amount of CTec2 bound to the unfibrillated BSKP (fibrillation time = 0) was significant because cellulose in the bleached pulp is highly accessible to cellulase. CTec2 binding curves for both BSKP and MSP fibrils were increased rapidly within the first hour of fibrillation suggesting rapid cell wall breakdown and further confirmed by SEM imaging (Figs. 1, 2). CTec2 binding to BKSP fibrils reached a plateau while binding to MSP fibrils increased slowly with further fibrillation. The cellulase binding curves shown in Fig. 7 are very similar to WRV curves (Fig. 5), confirming cellulase binding is directly related to accessible surface area as measured by WRV, in agreement with a recent study (Lee et al. 2010). The fact that CTec2 binding was near zero for the MSP sample at zero fibrillation time indicate: (1) external surface plays a minor role in cellulose accessibility (Luo and Zhu 2011; Sinitsyn et al. 1991; Wang et al. 2012a); (2) the MSP sample has limited pores accessible to cellulase due to lignin coverage (Leu and Zhu 2012; Wang et al. 2012c). The continued increase in CTec2 binding to MSP fibrils (Fig. 7) indicates mechanical fibrillation alone can break down cell wall to make cellulose completely accessible. It is simply a coincidence that the amount of CTec2 binding to the MSP fibrils is approximately the same as that bound to KSKP fibrils after extended fibrillation, e.g. 6 h. Because the amounts of cellulase binding shown in Fig. 6 include both the productive (to cellulose) and nonproductive (to lignin and other

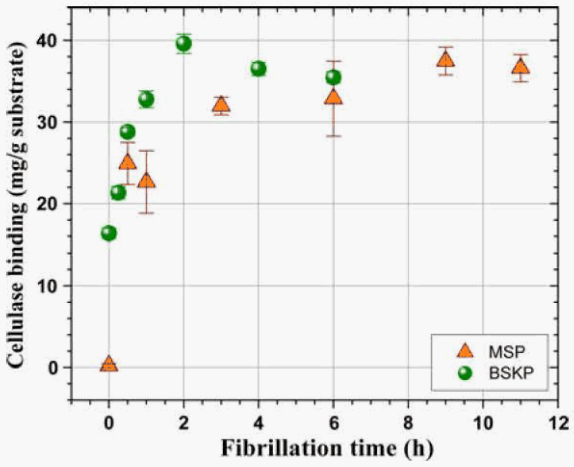

Fig. 7 Effect of fibrillation time on the amount of cellulase binding to fibrillated substrates

components), it is apparent that significantly more cellulase were bound productively to BSKP with zero lignin content and hemicellulose content of 15.1 % than to MSP that has a lignin content of 29.2 % and hemicellulose content of 16 % (Table 1). This explains the difference in SED between MSP and BSKP fibrils at the same CTec2 loading of 5FPU/g glucan (Fig. 3a, b).

Conclusions

Mechanical size reduction of plant biomass can be categorized into two classes: Class I reduces plant biomass to the level of fibers or fiber bundles with limited cell wall breakdown; Class II significantly breaks down fiber cell walls to produce macro or nanofibrils that renders cell wall highly or completely accessible to cellulase. Low degree of fibrillation, i.e., Class I size reduction, has a significant effect on enhancing enzymatic saccharification of a mechanical softwood pulp but with a overall low saccharification efficiency. This is because Class I size reduction merely increases fiber external surface without breaking down the cell wall structure and therefore with limited increase in cellulose accessibility evidenced by measured cellulase adsorption. Further fibrillation to the level of Class II size reduction significantly breaks down cell walls to macro or nanofibrils that made most fibrils accessible to cellulase resulting in significant saccharification of cellulose. The transition from Class I to Class II size reduction in the SuperMassCollider was rapid when the starting materials were wood fibers. Extended fibrillation has limited effect on cell wall breakdown as measured by water retention value and cellulase adsorption. This is probably due to the fact that fibrillation reached the limit of the stone used. Lignin plays a significant role in protecting cell wall. Under the same fibrillation energy input, the degree of cell wall breakdown for the mechanical softwood pulp is much less severer than that for a bleached softwood kraft pulp. The presence of lignin also prevented efficient cellulose saccharification by blocking cellulose as well as nonproductively binding to cellulase.

Acknowledgments This work was sponsored by the USDA Forest Service R&D special funding on Cellulose Nano-Materials (2012).

References

Agarwal UP, Reiner RS, Ralph SA (2010) Celulose I crystallinity determination using FT-Raman spectroscopy: univariate and multivariate methods. Cellulose 17(4):721–733

Ahola S, Turon X, Österberg M, Laine J, Rojas OJ (2008) Enzymatic hydrolysis of native cellulose nanofibrils and other cellulose model films: effect of surface structure. Langmuir 24(20):11592–11599

Besbes I, Alila S, Boufi S (2011) Nanofibrillated cellulose from TEMPO-oxidized eucalyptus fibres: effect of the carboxyl content. Carbohydr Polym 84(3):975–983

Bozell JJ, Petersen GR (2010) Technology development for the production of biobased products from biorefinery carbohydrates: the US department of energy's "top 10" revisited. Green Chem 12(4):539–554

Chai X-S, Zhu JY, Li J (2001) A simple and rapid method to determine hexeneuronic acid groups in chemical pulps. J Pulp Paper Sci 27(5):165–170

Cheng Q, Wang S, Rials TG, Lee SH (2007) Physical and mechanical properties of polyvinyl alcohol and polypropylene composite materials reinforced with fibril aggregates isolated from regenerated cellulose fibers. Cellulose 14(6):593-602

Dasari RK, Berson RE (2007) The effect of particle size on hydrolysis reaction rates and rheological properties in cellulosic slurries. Appl Biochem Biotechnol 137:289–299

Dekker J (2003) New insights in beating leading to innovative beating techniques. PIRA 2003 refining conference, Stockholm, Sweden

Endo T (2010) Bioethanol production from woods with the aid of nanotechnology. Synthesiology 4(2):270–281

Gupta R, Lee YY (2009) Pretreatment of hybrid poplar by aqueous ammonia. Biotechnol Prog 25:357–364

Hartman RR (1985) Mechanical treatment of pulp fibers for paper property development. In: Punton V (ed) The 8th fundamental research symposium: paper making materials.

Mechanical Engineering Publications Limited, Oxford, pp 413-442
Henriksson M, Berglund LA, Isaksson P, Lindström T, Nishino TD (2008) Cellulose nanopaper structures of high toughness. Biomacromolecules 9:1579–1585
Himmel ME, Ding SY, Johnson DK, Adney WS, Nimlos MR, Brady JW, Foust TD (2007) Biomass recalcitrance: engineering plants and enzymes for biofuels production. Science 315(5813):804–807
Hu F, Jung S, Ragauskas A (2012) Pseudo-lignin formation and its impact on enzymatic hydrolysis. Bioresour Technol 117:7–12
Iwamoto S, Nakagaito AN, Yano H (2007) Nano-fibrillation of pulp fibers for the processing of transparent nanocomposites. Appl Phys Mater Sci Process 89:461-466
Kallavus U, Gravitis J (1995) A comparative investigation of the ultrastructure of steam exploded wood with light, scanning and transmission electron-microscopy. Holzforschung 49(2):182–188
Kerekes RJ (2005) characterizing refining actions: linking the process to refining results. In: PIRA 2005 refining conference, Barcelona, Spain
Koo BW, Treasure TH, Jameel H, Phillips RB, Chang HM, Park S (2011) Reduction of enzyme dosage by oxygen delignification and mechanical refining for enzymatic hydrolysis of green liquor-pretreated hardwood. Appl Biochem Biotechnol 165(3-4):832–844
Laine J, Stenius P (1997) Effect of charge on the fiber and paper properties. Pap Puu 79:257–266
Lan TQ, Lou H, Zhu JY (2012) Enzymatic saccharification of lignocelluloses should be conducted at elevated pH 5.2-6.2. BioEner Res. doi:10.1007/s12155-012-9273-4
Lee SH, Chang F, Inoue S, Endo T (2010) Increase in enzyme accessibility by generation of nanospace in cell wall supramolecular structure. Bioresour Technol 101(19): 7218–7223
Leu S-Y, Zhu JY (2012) Substrate related factors affecting enzymatic saccharification of lignocelluloses: our recent understanding. BioEner Res. doi:10.1007/s12155-012-9276-1
Liu H Zhu JY, Chai XS (2011) In situ, rapid and temporally resolved measurements of cellulase adsorption onto lignocellulosic substrates by UV-vis spectrophotometry. Langmuir 27(1):272–278
Luo X, Zhu JY (2011) Effects of bine-induced fiber hornification on enzymatic saccharification of lignocelluloses. Enzym Microb Technol 48(1):92–99
Luo X, Gleisner R, Tian S, Negron J, Horn E, Pan XJ, Zhu JY (2010) Evaluation of mountain beetle infested lodgepole pine for cellulosic ethanol production by SPORL pretreatment. Ind Eng Chem Res 49(17):8258–8266
Luo X, Zhu JY, Gleisner R, Zhan HY (2011) Effect of wet pressing-induced fiber hornification on enzymatic saccharification of lignocelluloses. Cellulose 18:1339–1344
Mansfield SD, Mooney C, Saddler JN (1999) Substrate and enzyme characteristics that limit cellulose hydrolysis. Biotechnol Prog 15:804–816
Martin-Sampedro R, Filpponen I, Hoeger IC, Zhu JY, Laine J, Rojas OJ (2012) Rapid and complete enzyme hydrolysis of ligocellulosic nanofibrils. ACS Macro Lett 1(1): 1321–1325
Perlack RD, Wright LL, Turhollow A, Graham RL, Stokes B, Erbach DC (2005) Biomass as feedstock for a bioenergy and bioproducts industry: The technical feasibility of a billion-ton annual supply. Oak ridge national laboratory report, ORNL/TM-2005/66, US Dept of Energy
Segal L, Creely JJ, Martin AE, Conrad CM (1959) An empirical method for estimating the degree of crystallinity of native cellulose using the X-ray diffractometer. Text Res J 29:786–794
Sewalt VJH, Glasser WG, Beauchernin KA (1997) Lignin impact on fiber degradation.3. Reversal of inhibition of enzymatic hydrolysis by chemical modification of lignin and by additives. J Agric Food Chem 45(5):1823–1828
Sinitsyn AP, Gusakov AV, Vlasenko EY (1991) Effect of structural and physico-chemical features of cellulosic substrates on the efficiency of enzymatic hydrolysis. Appl Biochem Biotechnol 30:43–59
Siwiö J, Kärenlampil P (1998) Pits as natural irregularities in softwood fibers. Wood Fiber Sci 30:27–39
Spence KL, Venditti RA, Rojas OJ, Habibi Y, Pawlak JJ (2011) A comparative study of energy consumption and physical properties of microfibrillated cellulose produced by different processing methods. Cellulose 18(4):1097–1111
Sun Y, Cheng JY (2002) Hydrolysis of lignocellulosic materials for ethanol production: a review. Bioresour Technol 83(1):1–11
TAPPI (2009) TAPPI test methods. Technical Association of the Pulp and Paper Industry, Atlanta
Wang QQ, He Z, Zhu Z, Zhang Y-HP, Ni Y, Luo XL, Zhu JY (2012a) Evaluations of cellulose accessibilities of lignocelluloses by solute exclusion and protein adsorption techniques. Biotechnol Bioeng 109(2):381–389
Wang QQ, Zhu JY, Gleisner R, Kuster TA, Baxa U, McNeil SE (2012b) Morphological development of cellulose fibrils of a bleached eucalyptus pulp by mechanical fibrillation. Cellulose 19(5):1631–1643
Wang ZJ, Zhu JY, Gleisner R, Chen KF (2012c) Ethanol production form poplar wood the rough enzymatic saccharification and fermentation by dilute acid and SPORL pretreatments. Fuel 95:606–614
Weise U, Maloney T, Paulapuro H (1996) Quantification of water in difference states of interaction with wood pulp fibres. Cellulose 3:189–202
Zhu JY (2011) Physical pretreatment—woodybiomass sire-reduction—foforest biorefinery. In: Zhu JY, Zhang X, Pan XJ (eds) Sustainable production of fuels, chemicals, and fibers from forest biomass. American Chemical Society, Washington, pp 89–107
Zhu J, Wang G, Pan X, Gleisner R (2009a) Specific surface to evaluate the efficiencies of milling and pretreatment of wood for enzymatic saccharification. Chem Eng Sci 64(3):474-485
Zhu JY, Pan XJ, Wang GS, Gleisner R (2009b) Sulfite pretreatment (SPORL) for robust enzymatic saccharification of spruce and red pine. Bioresour Technol 100(8):2411–2418
Zhu W, Zhu JY, Gleisner R, Pan XJ (2010) On energy consumption for sire-reduction and yield from subsequent enzymatic sacchrification of pretreated lodgepole pine. Bioresour Technol 101(8):2782–2792

Zhu JY, Luo X, Tian S, Gleisner R, Negrone J, Horn E (2011a) Efficient ethanol production from beetle-killed lodgepole pine using SPORL technology and Saccharomyces cerevisiae without detoxification. Tappi J 10(5):9–18

Zhu JY, Verrill SP, Liu H, Herian VL, Pan XJ, Rockwood DL (2011b) On polydispersity of plant biomass recalcitrance and its effects on pretreatment optimization for sugar production. BioEner Res 4(3):201–210